Pérez-Lorente *et al. Journal of Biological Engineering* (2025) 19:28
https://doi.org/10.1186/s13036-025-00497-w

Journal of Biological Engineering

RESEARCH

Open Access

Engineering the T6SS of *Pseudomonas* for targeted delivery of antibacterial and antifungal effectors

Alicia Isabel Pérez-Lorente[1], Mario Araujo-Garrido[1], Antonio de Vicente[2], Diego Romero[1] and Carlos Molina-Santiago[1*]

Abstract

Background Bacteria employ diverse molecular systems, such as the type VI secretion system (T6SS) to outcompete other microorganisms and adapt to ecological niches. The T6SS is a versatile nanomachine capable of delivering toxic effectors into neighboring cells, providing advantages in bacterial interactions. In recent years, T6SSs have been proposed as promising tools for engineering selective antimicrobial platforms.

Results In this study, we successfully engineered *Pseudomonas putida* KT2440 to heterologously express and release T6SS effectors. The expression of Tse1, an effector from *Pseudomonas chlororaphis*, induced sporulation in plant-beneficial *Bacillus* strains via a T6SS-dependent mechanism, particularly when Tse1 was paired with a PAAR protein. Similarly, the engineered strain effectively inhibited *Aeromonas hydrophila* growth using the phospholipase toxin TplE from *Pseudomonas aeruginosa*. Furthermore, antifungal activity was achieved by coexpressing Tfe2, an effector from *Serratia marcescens*, with VgrGs, resulting in increased reactive oxygen species levels and cellular damage in *Botrytis cinerea*. Importantly, the T6SS was also employed to deliver non-T6SS effectors such as chitosanase, demonstrating its versatility in degrading fungal cell walls.

Conclusions Our findings demonstrate that the T6SS can be engineered to deliver both canonical and noncanonical effectors, providing a robust platform for targeted antibacterial and antifungal applications. The modularity of the system enables precise pairing of effectors with structural components such as VgrG and PAAR proteins, optimizing delivery efficiency. These engineered systems provide new opportunities for the development of biocontrol strategies in agriculture, microbiome modulation, and potential therapeutic applications. Future advancements in bioinformatics and protein engineering will further increase the specificity and functionality of T6SS-based delivery systems, offering innovative tools for managing microbial ecosystems and addressing global challenges in health and agriculture.

Keywords T6SS, *Pseudomonas putida*, Effectors, Antibacterial activity, Antifungal activity, Genetic engineering

*Correspondence:
Carlos Molina-Santiago
camolsan@uma.es
[1] Departamento de Microbiologia, Instituto de Hortofruticultura Subtropical y Mediterránea "La Mayora", Universidad de Málaga - Consejo Superior de Investigaciones Cientificas (IHSM-UMA-CSIC), Universidad de Málaga, Bulevar Louis Pasteur 31 (Campus Universitario de Teatinos), Málaga 29071, Spain
[2] Departamento de Microbiología, Universidad de Málaga, Bulevar Louis Pasteur 31 (Campus Universitario de Teatinos), Málaga 29071, Spain

Background

Bacteria in natural environments are constantly engaged in complex interactions, competing for resources, nutrients, or space to ensure their survival and dominance within their ecological niches [1, 2]. These interactions extend beyond bacteria to higher organisms such as plants, fungi, and humans, forming part of the broader framework of interkingdom interactions. For these competitive interactions, microorganisms have developed a

vast array of contact- and noncontact-dependent molecular tools, such as secondary metabolites, antimicrobial agents, secretion systems, and toxic effector proteins, that provide them with advantages under certain environmental conditions [3–5]. Among these tools, protein secretion systems are quite abundant in both Gram-negative and Gram-positive bacteria and have evolved to specialize in the secretion of different effectors and target cells [6]. For example, type 3 (T3SS) and type 4 (T4SS) secretion systems release unfolded effector proteins into eukaryotic host cells [7, 8], whereas type IX (T9SS) secretion systems are found in only some species of the phylum Bacteroidetes and are involved in bacterial movement (i.e., gliding movement of *Flavobacterium* by secreting adhesins in a T9SS dependent way) or used as a killing system to secrete virulence factors effectors by pathogenic strains [9]. Type 6 secretion systems (T6SSs) have been identified and described as sophisticated nanoweapons responsible for the delivery of effectors directly into neighboring cells [10], thus becoming an efficient antibacterial and anti-eukaryotic system [11–13]. Initially characterized in *Vibrio cholerae* [12] and *Pseudomonas aeruginosa* [11], T6SSs are known to be present in more than 25% of Gram-negative bacteria, comprising 13 core components that assemble into a versatile bacteriophage-like structure [14–17]. T6SSs have been reported to mobilize effectors against diverse targets, including Gram-negative and Gram-positive bacteria, fungi and other eukaryotic cells such as macrophages, epithelial cells or erythrocytes, among others [13, 18–21].

Structurally, the T6SS resembles a spear-like apparatus, with a baseplate serving as the specific site for a contractile sheath with a tube of effector-loaded proteins. At the tip of the apparatus, a trimeric VgrG spike and a PAAR protein facilitate the delivery of toxic effectors into target cells acting as carriers, ensuring that the effector payload reaches its destination. Upon activation by an unknown signal, the sheath contracts, propelling the Hcp tube, the VgrG-PAAR spike, and the corresponding effectors into neighboring target cells or the extracellular space [21–24]. Effector proteins can either directly connect with parts of the T6SS structure or be guided by tube-forming proteins, allowing for a diverse array of antibacterial and antieukaryotic activities [25–29]. The assembly of the T6SS relies on the coordinated interplay of VgrG, PAAR, and effector proteins, with specificity in effector delivery determined by VgrG proteins [30]. T6SS effector proteins can be classified into i) specialized (or evolved) effectors, which contain an N-terminal domain that is the structural component of the T6SS, such as VgrG, PAAR or Hcp, and a C-terminal effector domain; and ii) cargo effectors, which noncovalently interact with structural components of the T6SS, such as VgrG, PAAR or Hcp [31–33]. Importantly, the toxicity of the system is driven primarily by the effectors, since the damage caused by the puncture itself appears negligible [34, 35].

In recent years, engineered T6SSs have been proposed as versatile and selective antimicrobial tools, offering promising strategies to combat antibiotic resistance in microbial pathogens [36]. Few studies in this field have demonstrated the potential of engineered T6SSs to kill a variety of bacteria by delivering toxic effectors. For example, Hersch and collaborators [37] employed *Vibrio cholerae* to deliver Cre recombinase via the T6SS, whereas research conducted by Jana and colleagues [36] highlighted the construction of a modular and inducible antibacterial toxin delivery platform using a T6SS controlled by an externally induced switch in *Vibrio natriegens* with potential applications in marine research. Additionally, innovative strategies employing a constitutively active T6SS in *Enterobacter cloacae* have been explored for targeted bacterial killing within mixed communities [38]. In this context, the exploration of T6SS-based strategies represents a promising avenue for combating pathogens in different fields.

One of the key points to address is the selection of the delivery bacterium. In this study, we engineered *Pseudomonas* strains as inducible platforms for the delivery of antifungal and antibacterial effectors, targeting both Gram-positive and Gram-negative bacteria and fungi. As a proof of concept, we used mainly *Pseudomonas putida* KT2440 as the delivery bacterium. This strain, which encodes three T6SSs in its genome [39], has demonstrated great potential in metabolic engineering [40, 41] and meets the requirements to serve as an optimal delivery bacterium: i) KT2440 is a good colonizer of the rhizosphere of many plants, a potential ecological niche for the application of this system; ii) it is metabolically diverse and easy to manipulate; and iii) multiple genetic tools, such as SEVA plasmids, have been specifically developed for this strain [42].

To test the system, we analyzed combinations of different genetic elements, such as promoters, VgrGs and effectors, all of which were combined in plasmids and heterologously expressed in the delivery bacterium. We selected VgrGs or PAARs from *P. putida* KT2440, *Pseudomonas* sp. 250 J, *P. chlororaphis* and *Serratia marcescens* and combined them with their specific effectors, just as they are linked in the bacterial strain of origin, or with other nonrelated effectors, followed by evaluation of the functionality and specificity of the combinations. This proof-of-concept engineered bacterial system demonstrated the feasibility of applying inducible and customizable antimicrobial properties in agriculture and other fields, introducing activities such as sporulation induction in *Bacillus* species by the Tse1 effector from

P. chlororaphis, the antibacterial activity of TplE from *P. aeruginosa*, the antifungal activities of the Tfe2 effector from *S. marcescens*, and the activity of non-T6SS-related proteins such as chitosanase from *B. subtilis*, thus offering promising strategies for advanced genetic programming and the development of targeted antibacterial strategies.

Methods

Strains, media and culture conditions

A complete list of the bacterial strains used in this study is shown in Suppl. Table 1. The bacterial cells were routinely grown in liquid lysogeny broth (LB) medium at 28 °C (for *Pseudomonas* strains, *S. marcescens, A. hydrophila* and *Bacillus* strains) or 37 °C (for *Escherichia coli*) with shaking on an orbital platform. *B. cinerea* was routinely grown on potato dextrose agar (PDA) or potato dextrose broth (PDB) at 28 °C. When necessary, antibiotics, 1 mM 3-methylbenzoate (3-MB) and 1 mM isopropyl β-D-thiogalactopyranoside (IPTG) were added to the media at appropriate final concentrations (gentamicin, 60 μg/ml; kanamycin, 50 μg/ml; rifampicin, 100 μg/ml).

General DNA manipulation techniques

DNA manipulation was performed using commercial kits: Plasmid DNA was prepared using the QIAprep Spin Miniprep Kit (Qiagen, Inc., Valencia, CA) following manufacturing instructions. When needed, DNA was purified via the GFX™ PCR DNA and Gel Band Purification Kit. The oligonucleotides used in this work are indicated in Suppl. Table 2. Colony PCR was performed by transferring cells with a sterile toothpick directly from fresh agar plates into PCR tubes. The suitability of the constructs was confirmed via DNA sequencing.

Plasmid construction

Plasmids were constructed via Gibson assembly [43]. A list of the plasmids used in this manuscript is shown in Table 1. Briefly, *vgrG*, *paar* and effector genes were amplified by PCR separately or in combination, depending on the genomic context, and purified for subsequent steps. The pSEVA234 (named as p234) and pSEVA238 (named as p238) inducible expression plasmids (pBBR1 origin of replication) and pSEVA2213 (named as p2213) constitutive expression plasmid (carrying pEM7 promoter and RK2 origin of replication) were digested with the restriction enzyme EcoRI or HindIII and mixed with the PCR-amplified fragments, and Gibson assembly was performed for 1 h at 60 °C. The primers used for the amplification of the effectors *vgrG* and *paar* incorporated the RBS sequence into the Gibson constructs (5´-AAGGAG TCTAGACC- 3´). Five microliters of each of the Gibson reaction mixtures was transformed into *E. coli* CC118 cells, and selection was performed on LB-Km plates, obtaining the plasmids p234/p2213 harboring *vgrG/paar*, effector genes or a combination of both. The constructs were separately transformed into *P. putida* KT2440 or *Pseudomonas* sp. 250 J by electroporation [44], followed

Table 1 Plasmids used in this work

Plasmid	Description[a]	Source or reference
pRL662-gfp2	Broad host range vector derived from pBBR1MCS- 2 expressing a green fluorescence protein (gfp); Gm^R	Erh-Min Lai collection
pSEVA234 (p234)	Expression vector: oriV(pBBR1) lacI-Ptrc; inducible by IPTG; Km^R	SEVA collection
pSEVA238 (p238)	Expression vector: oriV(pBBR1) XylS-Pm; inducible by 3-Methylbenzoate; Km^R	SEVA collection
p234-Tse1	pSEVA234 carrying *tse1* gene from *P. chlororaphis* PCL1606; Km^R	**This work**
p234-PAAR	pSEVA234 carrying *PAAR* gene from *P. chlororaphis* PCL1606; Km^R	**This work**
p234-PAAR-Tse1	pSEVA234 carrying *paar-tse1* gene from *P. chlororaphis* PCL1606; Km^R	**This work**
p238-VgrGkt4	pSEVA238 carrying *vgrG4* gene from *P. putida* KT2440; Km^R	**This work**
p238-VgrGkt4-TplE	pSEVA238 carrying *vgrG4* gene from *P. putida* KT2440 and *PA1508-PA1510* from *P. aeruginosa* PAO1; Km^R	**This work**
p234-VgrG1	pSEVA234 carrying *vgrGsma* gene from *S. marcescens*; Km^R	**This work**
p234-VgrG2	pSEVA234 carrying *vgrGsmb* gene from *S. marcescens*; Km^R	**This work**
p234-Tfe2	pSEVA234 carrying *tfe2* gene from *S. marcescens*; Km^R	**This work**
p234-VgrG1-Tfe2	pSEVA234 carrying *vgrGsma* and *tfe2* genes from *S. marcescens*; Km^R	**This work**
p234-VgrG2-Tfe2	pSEVA234 carrying *vgrGsmb* and *tfe2* genes from *S. marcescens*; Km^R	**This work**
pSEVA2213 (p2213)	Expression vector: oriV(RK2) pEM7, Km^R	SEVA collection
p2213-VgrG250 J	pSEVA2213 carrying *vgrG250 J* gene from *Pseudomonas* sp. 250 J; Km^R	**This work**
p2213-VgrG2a-csn	pSEVA2213 carrying *vgrGkt* gene from *P. putida* KT2440 and *csn* gene from *B. subtilis* NCIB3610; Km^R	**This work**
p2213-VgrG250 J-csn	pSEVA2213 carrying *vgrG250 J* gene from *Pseudomonas* sp. 250 J and *csn* gene from *B. subtilis* NCIB3610; Km^R	**This work**

[a] Gm^R, Km^R, Rif^R, and Nal^R, resistance to gentamycin, kanamycin, rifampicin, and nalidixic acid, respectively

by selection on LB-Km plates, and the strains *P. putida* KT2440 and *Pseudomonas* sp. 250 J carrying the constructed plasmids were obtained. The integrity of the constructs described above, either in *E. coli* or *P. putida*, was checked via miniprep, restriction and agarose gel visualization. In addition, plasmid sequencing was performed at STABvida for plasmid confirmation.

Bacterial competition and intoxication assays

Bacillus subtilis NCIB 3610, *Bacillus velezensis* FZB42, *A. hydrophila* DSM30187 and *Pseudomonas* strains were cultured on LB plates overnight at 28 °C, and the resulting colonies were subsequently cultured overnight in 5 ml of LB at 28 °C on an orbital shaker before normalization to OD_{600} = 3.0 in 1 ml of sterile distilled water (Suppl. Figure 1). The attacker and prey strains were mixed at a 1:1 ratio, and 5 µL drops were spotted onto LB plates, which were incubated at 28 °C for 4 h (*A. hidrophyla* DSM30187 killing assays) or 24 h (*B. subtilis* NCIB 3610 *and B. velezensis* FZB42 sporulation assays). The resulting colonies were resuspended in 1 ml of sterile distilled water, serially diluted and plated on LB medium. Next, *Bacillus* cells were selected at 40 °C, and CFUs were enumerated after 24 h. *Aeromonas* cells were selected on the basis of rifampicin resistance, as the *Aeromonas* strain used was previously treated with mutagens and had acquired rifampicin resistance.

For competition assays against fungi, *B. cinerea* was cultured from a germinated conidial suspension by incubation in PDB (Oxoid) inoculated with a spore suspension at 28 °C for 24 h at 150 rpm. The *Pseudomonas* strains were cultured on LB plates overnight at 28 °C, and the resulting colonies were subsequently cultured overnight in 5 ml of LB at 28 °C on an orbital shaker. Subsequently, 5–10 germinated hyphae (macrocolonies) were mixed with 40 µL of bacterial culture in 24-well plates containing PDB at 28 °C overnight at 150 rpm.

Sporulation assays

Spots of bacteria were resuspended in 1 ml of sterile distilled water. Then, serial dilutions were prepared and cultured in LB solid medium for determination of vegetative cell CFU counts. Afterward, the same serial dilutions were heated at 80 °C for 10 min to kill vegetative cells and immediately cultured again on LB solid medium. The plates were grown overnight at 28 °C, and the resulting colonies were counted to calculate the percentage of *B. subtilis* sporulation (%).

Protein–protein interaction *in silico* analyses

To predict the three-dimensional structure of the protein complex, we employed AlphaFoldSever. The amino acid sequences, in FASTA format, of the two proteins of interest were retrieved from protein databases. Sequences were processed through AlphaFold 3.0 using the ColabFold implementation, which enables the modeling of both individual protein structures and protein–protein complexes. Model confidence was assessed using the predicted aligned error (PAE) and confidence scores (pLDDT and interface pTM scores). To further investigate interaction specificity and identify key interface residues, AlphaBridge, a computational tool for protein–protein docking refinement, was applied to the selected AlphaFold 3.0 models. The AlphaFold-predicted structures were used as input for AlphaBridge, which evaluates residue-residue interactions within the predicted binding interface and calculates the interaction energy landscape and identified residue pairs with high likelihood of forming stable contacts.

Measurement of reactive oxygen species (ROS) levels

The intracellular ROS levels were measured by staining with dihydrorhodamine 123 (DHR123; Sigma). Following incubation, DHR123 was added to the cell suspension at a final concentration of 2 µg/ml, and the mixture was incubated for 5 min at room temperature. The cells were counterstained with the lipophilic dye FM4 - 64 (Thermo Fisher) to stain the plasma membrane. Images were obtained using a Leica Stellaris 8 confocal microscope with a 63 × NA 1.3 Plan APO oil-immersion objective, with excitation at 488 nm and emission detection between 510 and 580 nm (for DHR123 fluorescence emission) and between 670 and 850 nm (for FM4 - 64 fluorescence emission). Image processing and signal intensity measurements were performed using FIJI/ImageJ software [45]. For each experiment, the laser settings, scan speed, HyD detector gain, and pinhole aperture were kept constant across all acquired images.

Chitosan level quantification

Changes in the chitosan composition were determined via eosin Y labeling. The samples were subsequently resuspended in citrate–phosphate buffer (0.2 M NaH_2PO_4, 0.1 M K citrate; pH 6) at a final eosin Y concentration of 1 µg/ml. After 10 min of incubation at room temperature, the cells were washed two times with citrate–phosphate buffer and placed on 1% agarose pads. Finally, the stained cells were imaged using an excitation wavelength of 488 nm, with emission detected between 510 and 640 nm. Images were obtained via a Leica Stellaris 8 confocal microscope with a 63 × NA 1.3 Plan APO oil-immersion objective. Processing and signal intensity were performed via FIJI/ImageJ software [45]. For each experiment, the laser settings, scan speed, HyD detector gain, and pinhole aperture were kept constant across all acquired images.

Transmission electron microscopy (TEM)

B. cinerea samples were fixed in a solution containing 2.5% (v/v) glutaraldehyde and 4% (v/v) paraformaldehyde overnight at 4 °C. Following three washes in the fixation mixture, the samples were postfixed with a 1% osmium tetroxide solution for 90 min at room temperature, followed by two additional washes and stepwise dehydration with an ethanol gradient (30%, 50%, 70%, 90%, and 100% twice). During the transition from 50 to 70% ethanol, the samples were immersed in a 2% uranyl acetate solution in 50% ethanol at 4 °C overnight. After dehydration, the samples were gradually infiltrated with low-viscosity Spurr's resin, with a resin-to-ethanol ratio of 1:1, for 4 h, followed by a ratio of 3:1 for another 4 h, and finally, with pure resin overnight. The sample blocks were then encapsulated in molds with pure resin and left to polymerize for 72 h at 70 °C. Once dried, the samples were examined via a JEOL JEM- 1400 transmission electron microscope at an accelerating voltage of 80 kV.

Statistical analysis

The results are expressed as the mean ± standard error of the mean (SEM). Statistical significance was assessed via ANOVA or Student's t tests. All analyses were performed via GraphPad Prism® version 9 or Microsoft Excel. P values <0.05 were considered indicative of statistical significance. Asterisks indicate the level of statistical significance: $^{*}p<0.05$, $^{**}p<0.01$, $^{***}p<0.001$, and $^{****}p<0.0001$.

Results

Engineered *Pseudomonas* strainsinduced *Bacillus* sporulationviaT6SSs

Fundamental insights gained in recent years have allowed the development of hypotheses regarding a T6SS genetically engineered for the delivery of effectors. We aimed to develop a proof of concept for the construction of a genetically engineered bacterial strain that could transcriptionally regulate and control the proper release of cargo effectors in a T6SS-dependent manner as an alternative to classic biocontrol strategies. For this purpose, we i) studied the feasibility of controlling the expression of exogenous cargo effectors in a delivery bacterium and ii) analyzed the efficacy of the effectors after coexpressing them with different VgrG or PAAR proteins, leading to their release by functional T6SSs present in the delivery strains.

In a previous study, we revealed that Tse1 from *P. chlororaphis* is a hydrolase effector that induces the sporulation of *B. subtilis* [20]. Tse1 is genomically linked to a *paar* gene in *P. chlororaphis*. As a first stage in the design of a versatile delivery effector system, we demonstrated the heterologous expression of Tse1 in KT2440 and tested the functionality of the system by measuring sporulation induction in *Bacillus* strains that have beneficial effects on plants. To control the expression of the constructs carrying Tse1 effector and/or PAAR protein, we employed the inducible p234 plasmid, which carries a LacIq-Ptrc promoter inducible by IPTG (Suppl. Figure 2 A). The KT2440 WT strain and KT2440 strains carrying the p234, p234-PAAR, p234-Tse1 and p234-PAAR-Tse1 plasmids were tested in competition experiments against *B. subtilis* NCIB3610 or *B. velezensis* FZB42. With these assays, we intended, first, to evaluate the activity of Tse1 expressed in a different genetic background and, second, the ability of the PAAR protein from *P. chlororaphis* to release the toxin correctly. A significant reduction in *B. subtilis* sporulation from 11.7% (when grown alone) to 1.88% was detected when the bacterium was in competition with *P. putida* KT2440 (Fig. 1A), and a reduction to 5.2% when KT2440 was carrying an empty p234 plasmid. This decrease was consistent when *P. putida* carried both the empty p234 plasmid, p234-PAAR and p234-Tse1. However, during the competition of *B. subtilis* with a KT2440 strain coexpressing *paar* and *tse1* (KT2440 p234-PAAR-Tse1), *B. subtilis* sporulation levels significantly increased to 20.2%, 1.72-fold greater than the sporulation levels observed when *B. subtilis* was grown alone, 3.88-fold greater that the sporulation when competing against KT2440 (p234) and ten-fold greater than the sporulation observed in the case of competition against KT2440 WT (Fig. 1A). This induction of sporulation was also observed during the interaction of KT2440 (p234-PAAR-Tse1) with *B. velezensis* FZB42 (two-fold sporulation increase) (Fig. 1B). However, in this case, we did not observe a reduction in FZB42 sporulation levels in competition with KT2440 WT or KT2440 (p234). To confirm that the sporulation induction was T6SS dependent, p234-PAAR-Tse1 plasmid was also transformed into a *P. putida* KT2440 strain depleted of three T6SSs encoded in its genome (KT2440 Δ3T6SS). Results obtained for *B. subtilis* and *B. velezensis* after competing with KT2440 Δ3T6SS (p234-PAAR-Tse1) showed sporulation levels similar to those provoked by KT2440 Δ3T6SS, KT2440 WT or KT2440 WT (p234) (Fig. 1A and 1B).

Therefore, our results demonstrated that engineered KT2440 induce *Bacillus* sporulation via the activity of the T6SS. These results also confirm the need to combine Tse1 with a PAAR protein for the correct release of the effector mediated by a T6SS into the target cell and the induction of *Bacillus* sporulation by the Tse1 effector, since the sole expression of *tse1* via the PAAR proteins from KT2440, encoded in its genome, failed to induce *Bacillus* sporulation.

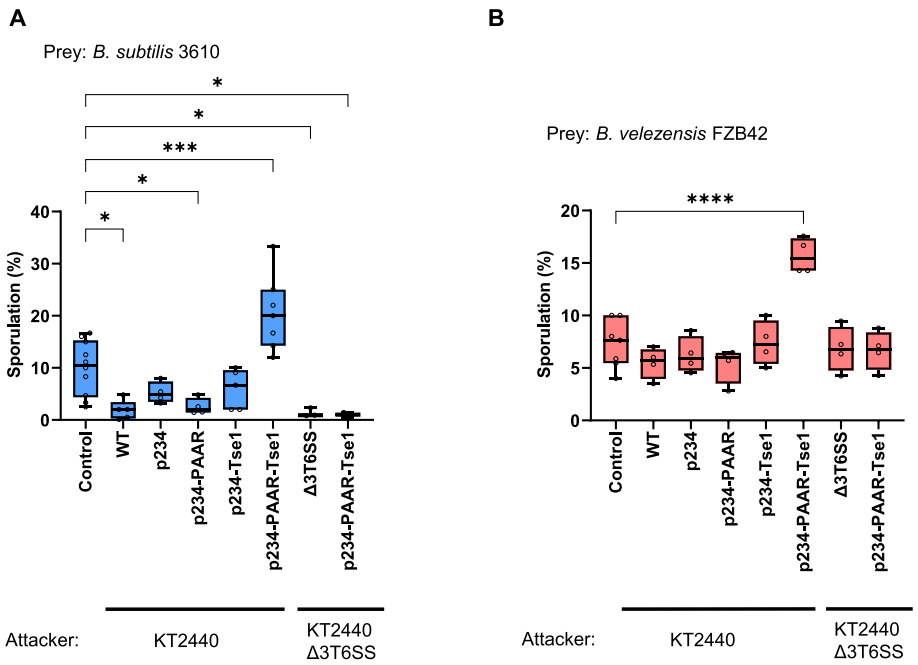

Fig. 1 Engineering *P. putida* for sporulation induction of *Bacillus* strains. **A** Competition assays. Quantification of *Bacillus* subtilis NCIB 3610 sporulation growing alone and in competition with the KT2440 WT or KT2440 Δ3 T6SS strains carrying different plasmids (p234, p234-PAAR, p234-Tse1, and p234-PAAR-Tse1) as attackers. **B** Competition assays. Quantification of *Bacillus velezensis* FZB42 sporulation growing alone and in competition with the KT2440 WT or KT2440 Δ3T6SS strains carrying different plasmids (p234, p234-PAAR, p234-Tse1, and p234-PAAR-Tse1) as attackers. For all the experiments, at least three biological replicates are shown, and the error bars represent the SDs. Statistical significance was assessed via one-way ANOVA. *p value < 0.1, ** p value < 0.01

Aeromonas death is achieved by engineered *Pseudomonas* strains via T6SS-dependent heterologous toxin expression

Once we demonstrated that the T6SS could be engineered for heterologous delivery of a toxin against *Bacillus*, we tested the versality of the system against Gram-negative bacteria. Most T6SS-related toxins have been reported to be active against Gram-negative bacteria [22]. We selected the well-studied toxin TplE from *P. aeruginosa* PAO1, which has been described as an antibacterial toxin with phospholipase activity that targets the periplasmic region of bacteria, causing cell death [46]. The activity of TplE was tested in combination with a VgrG from KT2440. The gene *PP3386* (named VgrGkt4), encoding a VgrG from *P. putida* KT2440, was combined with the genes *PA1508-PA1510* from *P. aeruginosa* PAO1, encoding the lipase toxin TplE (*PA1510*), the antitoxin TplEi (PA1509) and the gene *PA1508*, which is a PAAR3 protein. For this construct (p238-VgrGkt4-TplE), we used the p238 plasmid, which harbors the XylS-Pm promoter which is induced by 3-MB (Suppl. Figure 2B). With the aim of providing more confidence to this VgrG-effector combination, we tested the use of in silico modelling tools to evaluate the probable link between VgrGkt4 trimers and TplE (Fig. 2). The use of Alphafold3 [47] in combination with Alphabridge [48] was employed to predict interacting residues between the proteins. The results revealed the expected three-dimensional structure of VgrGkt4-TplE complexes (Fig. 2A), and the interaction between VgrGkt4 proteins (Fig. 2B). This interaction is produced mainly due to the binding between amino acids from TplE located in positions 23–33 and 38–45 and those located in the positions 773–783 and 821–828 of the subunit A of the VgrG trimer analyzed (Fig. 2C). Increasing cut-off for interface detection assessed the interaction specifically to amino acids Pro- 24, Val- 25 and Tyr- 26 of TplE with Ile- 826, Arg- 827 and Ile- 828.

The constructs were transformed into KT2440, and competition assays were performed against *A. hydrophila* DSM 30187, a bacterial strain belonging to the *Aeromonas* genera which are considered as ubiquitous pathogenic microorganisms found in soils, plants and aquatic environments [49]. The survival rates of the prey strain revealed a reduction in the viability of *A. hydrophila* in competition with KT2440 (VgrGkt4-TplE) in comparison with that of *Aeromonas* in competition with KT2440 WT or KT2440 carrying the empty p238 or p238-VgrGkt4 vector (Fig. 2D). To confirm that the antibacterial activity was T6SS dependent, plasmids carrying the TlpE effector were also transformed into

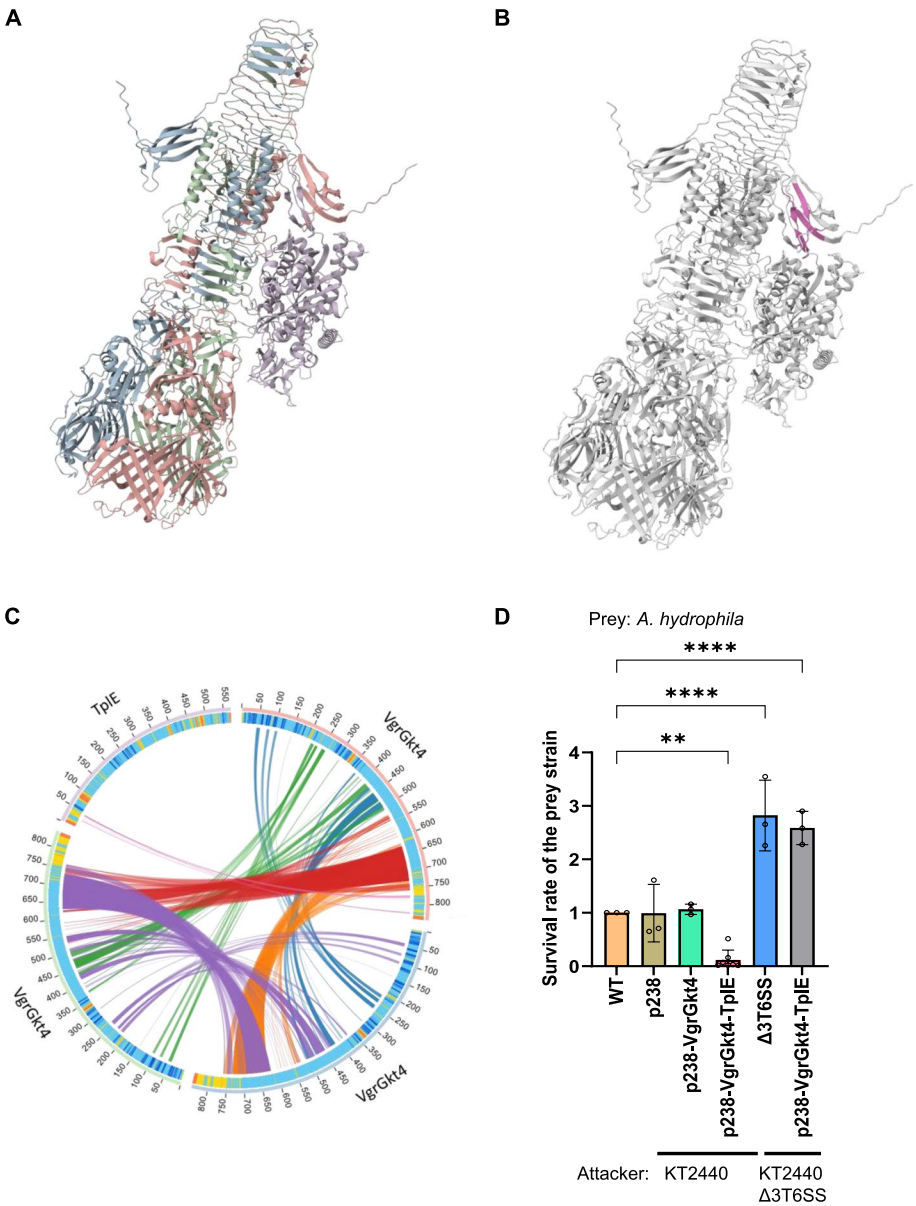

Fig. 2 In silico prediction and experimentally engineering of *P. putida* KT2440 to kill *A. hydrophila* via T6SS-dependent heterologous effector expression. **A** Three-dimensional view of the conformational structure of a VgrGkt4 trimer (depicted in blue, red and green) with a monomer of the TplE effector (depicted in purple). **B** Three-dimensional view of the VgrGkt4-TpleE complex highlighting the residues of TplE involved in the linking with VgrGkt4. Representation was obtained using Alphaphold3 to develop a 3D model and Alphabridge to highlight residues involved in the interaction between proteins. **C** Alphabridge diagram showing all the interactions between the proteins of the model. Each color represents interactions between different pairs of proteins. **D** Survival rate of *A. hydrophila* DSM 30187 (prey) in competition with KT2440 WT or KT2440 Δ3T6SS strains carrying different plasmids (p238, p238-VgrGkt4 and p238-VgrGkt4-TplE) as attackers. For all the experiments, at least three biological replicates are shown, and the error bars represent the SDs. Statistical significance was assessed via one-way ANOVA. ** p value < 0.01, *** p value < 0.001, **** p value < 0.0001

KT2440 Δ3 T6SS. The performance of *Aeromonas* was better when the T6SS was not functional, both in the presence and in the absence of TplE, thus demonstrating that TplE inhibitory activity was dependent on a functional T6SS (Fig. 2D).

Overall, we conclude that KT2440 can be effectively equipped with novel antibacterial effectors that target Gram-positive or Gram-negative bacteria and that VgrG proteins can be successfully paired with effectors from other microbial sources to increase antibacterial activity.

An engineered T6SS expressing Tfe2 exhibited antifungal activity against *Botrytis cinerea*

After successful engineering of the T6SS to target different bacterial species, we proceeded to evaluate its potential in interkingdom competition against fungi. To test this hypothesis, we selected *B. cinerea* as the fungal prey because of its significance as an agricultural phytopathogen [50, 51]. To date, only three T6SS effectors have been described as antifungal agents [18, 52], with Tfe1 and Tfe2 from *S. marcescens* being the first two T6SS antifungal effectors reported. Specifically, Tfe2 has been shown to inhibit fungal growth by disrupting nutrient uptake and amino acid metabolism, leading to the induction of autophagy when it is expressed in *Saccharomyces cerevisiae* and *Candida albicans*. However, the authors did not identify any *vgrG*, *paar* or *hcp* genes upstream of this effector [17].

To test the activity of this cargo effector in our genetic system, we selected two orphan *vgrG* from *S. marcescens* (called *vgrG1* and *vgrG2*) that were not genomically close to *tfe2*. We developed a series of inducible plasmids: control plasmids expressing only the VgrG proteins or the Tfe2 effector (p234-VgrG1, p234-VgrG2, and p234-tfe2) and those with a combination of each *vgrG* with *tfe2* (p234-VgrG1-tfe2 and p234-VgrG2-tfe2). With these combinations, we aimed to test the possible antifungal activity of the selected VgrGs and the necessity of coexpressing VgrG with Tfe2 for antifungal activity. Once all the constructs were generated, they were transformed into *P. putida* KT2440, and competition experiments against *B. cinerea* were performed in PDB supplemented with IPTG for induction of expression.

We first analyzed the interaction between *P. putida* KT2440 WT and *B. cinerea* and observed that KT2440 did not have a detrimental effect on *B. cinerea* growth, highlighted by the absence of reactive oxygen species (ROS) and of changes in the cellular structure of *B. cinerea* after 24 h of competition (Fig. 3A and B). We next performed competition assays between *B. cinerea* and KT2440 carrying the expression systems described above. Our results confirmed that, in our bacterial system, Tfe2 requires coexpression of a VgrG to have antifungal effects. In fact, neither the VgrGs nor Tfe2 exhibited antifungal properties when expressed alone, showing no inhibition of *B. cinerea* growth or induction of ROS production in *B. cinerea* after 24 h of competition (Fig. 3A and B). However, the coexpression of Tfe2 with any of the two VgrGs used in this system resulted in a significant increase in ROS production, represented by an increase in the number of cells positively responding to the dihydrorhodamine 123 signal (Fig. 3A and B). This increase in ROS production was consistent with the increase in cell death (Fig. 3A and Suppl. Figure 3), as noted by the localization of the FM4 - 64 dye, which is used to stain cell membranes, in the cytoplasm of dead cells. KT2440 Δ3 T6SS strains carrying expression plasmids were also assayed in competition experiments against *B. cinerea* (Suppl. Figure 4 A and B). Results confirmed the T6SS-dependency of the damage observed by Tfe2 as no cell death nor ROS induction was detected by confocal laser scanning microscopy (CLSM). To confirm the damage inflicted, TEM analyses of *B. cinerea* cells in competition with KT2440 coexpressing VgrG1 and Tfe2 revealed cellular damage, vacuolization, degraded organelles and aggregates of dense material, all of which indicated cell stress and death (Fig. 3C). Therefore, these findings demonstrated that the heterologous expression of VgrG and Tfe2 in KT2440 provides this strain with antifungal capacity, at least against *B. cinerea*. In addition, we demonstrated the possibility of combining Tfe2 with different VgrGs to secrete the effector via the T6SS and the need for the coexpression of both elements to achieve the antifungal effects of Tfe2.

Secretion of non-T6SS-dependent effectors via T6SSs

We have shown that the functional combination of different VgrGs with T6SS effectors provides KT2440 with antibacterial and antifungal properties. We next investigated the feasibility of combining T6SSs with other proteins not directly related to the T6SS. Specifically, and for continued research on interkingdom interactions between bacteria and fungi, we selected a chitosanase from *B. subtilis* and studied its activity against *B. cinerea*. Chitosanase acts by catalyzing the hydrolysis of β−1,4-glycosidic bonds in chitosan, a major component of the fungal cell wall, converting it into chitooligosaccharides [53]. To assess the possibility of the secretion of chitosanase via the T6SS in the KT2440 delivery strain and to provide this strain with antifungal capacity, we constructed constitutive expression plasmids (using p2213 as backbone plasmid) in which two different VgrGs were combined with the chitosanase (Csn) from *B. subtilis:* VgrG250 J from *Pseudomonas* sp. 250 J and VgrG2a from *P. aeruginosa* PAO1 (plasmids p2213-VgrG250 J-csn and p2213-VgrG2a-csn). The selection of these two VgrGs was based on their distinct phylogenetic and functional characteristics, which allowed us to explore the versatility and specificity of T6SS-mediated effector secretion. While VgrG2a, is associated with the H2-T6SS, a system that is phylogenetically distinct from the three T6SSs present in *P. putida* KT2440; VgrG250 J was selected because this strain encodes a T6SS that belongs to the same family as one of the T6SSs in *P. putida* KT2440. These plasmids were transformed into the KT2440 WT strain, and competition assays were performed against *B. cinerea* (Fig. 4). To assess the effects of the constructs on

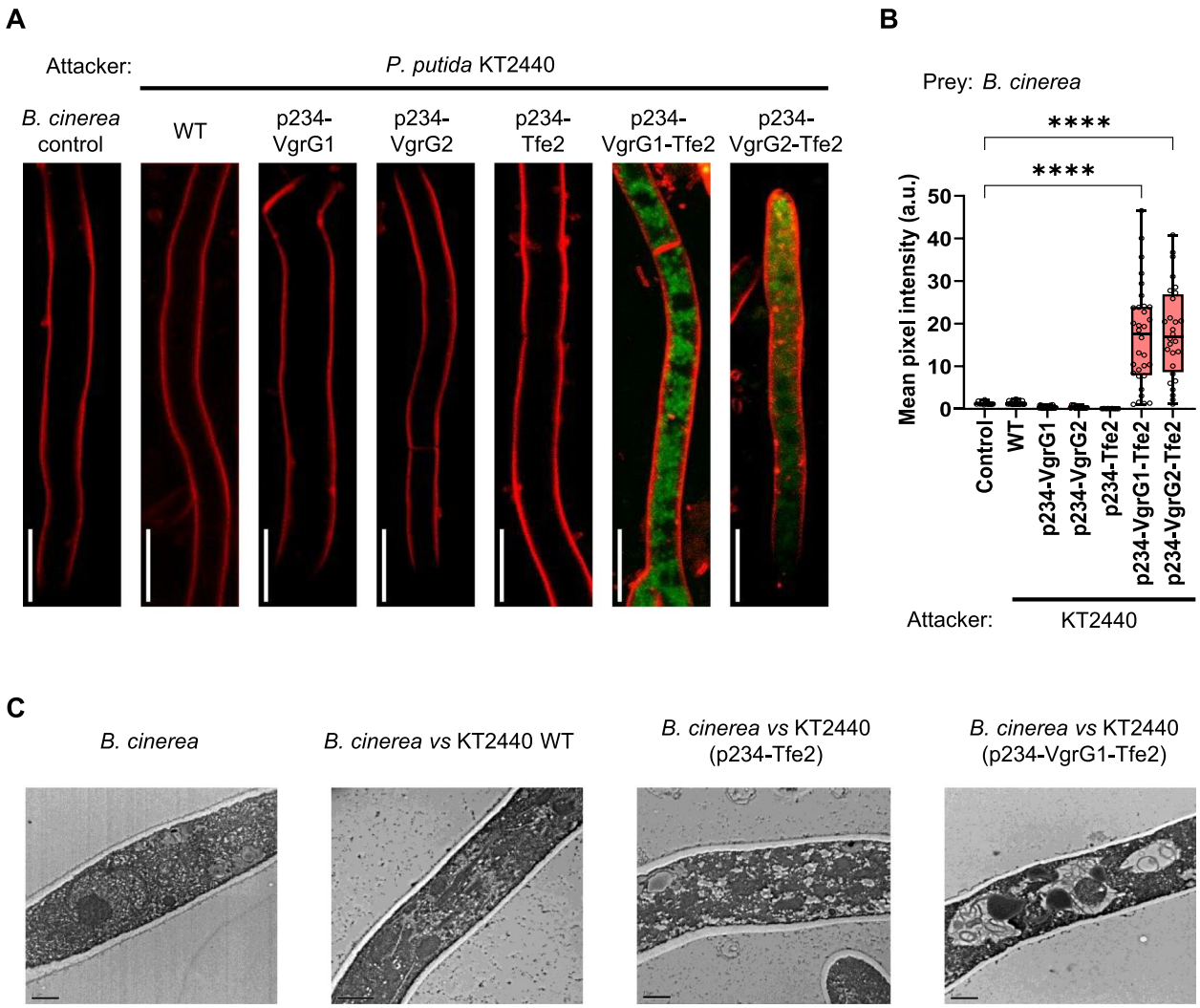

Fig. 3 Interkingdom competitions mediated by T6SS effectors. **A** CLSM of *B. cinerea* hyphae after competition with the *P. putida* KT2440 WT strain or strains carrying plasmids (p234-VgrG1, p234-VgrG2, p234-Tfe2, p234-VgrG1-Tfe2, and p234-VgrG2-Tfe2) as attackers. The samples were treated with FM4 - 64 and DHR123 to stain the fungal membrane and reactive oxygen species, respectively. Scale = 10 µm. **B** Box-and-whisker plot showing the mean ROS pixel intensity (a.u.) of *B. cinerea* (prey) growing alone and in competition with the KT2440 WT strain and strains carrying plasmids (p234-VgrG1, p234-VgrG2, p234-Tfe2, p234-VgrG1-Tfe2, and p234-VgrG2-Tfe2) as attackers. In all the experiments, at least three biological replicates are shown, and the error bars represent the SDs. Statistical significance was assessed via one-way ANOVA. **** *p* value < 0.0001. **C** TEM analysis of *B. cinerea* (prey) growing alone and in competition with the KT2440 WT strain and strains carrying plasmids (p234-Tfe2 and p234-VgrG1-Tfe2). Scale = 1 µm

the degradation of chitosan, we quantified staining with eosin Y, a dye that specifically stains chitosan on fungal cell walls [54]. We initially determined that KT2440 WT did not have a detrimental effect on chitosan degradation alone, thus permitting the correct evaluation of the potential effects of our constructs. A comparison of *B. cinerea* with KT2440 coexpressing VgrG2a and Csn revealed no degradation of chitosan. However, a reduction in the eosin Y signal and, therefore, degradation of chitosan was observed when *B. cinerea* was in competition against KT2440 coexpressing VgrG250 J and Csn (Fig. 4A and B). These results confirm that chitosanase from *B. subtilis* affects *B. cinerea* chitosan and that this effect does not occur with any combination of chitosanase and VgrG proteins, occurring only with specific combinations, such as VgrG250 J and chitosanase. In addition, to eliminate any antifungal activity of VgrG250 J, and more specifically affect the chitosan from *B. cinerea*, we expressed VgrG250 J alone in KT2440 WT, and the results revealed no reduction in eosin Y levels, thus confirming that VgrG250 J did not present chitosanase activity (Fig. 4A and B).

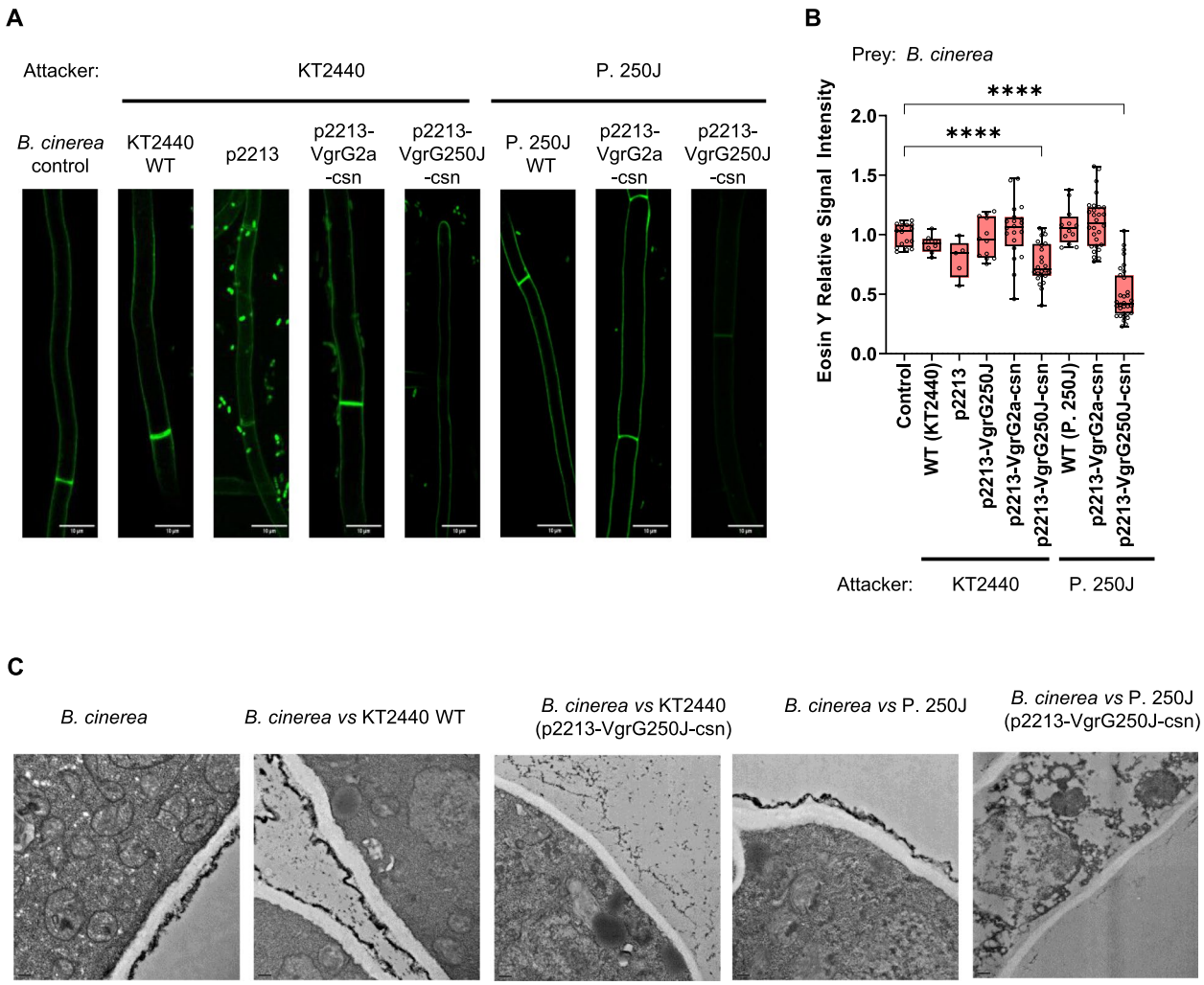

Fig. 4 Interkingdom competitions mediated by non-T6SS-dependent effectors. **A** CLSM of *B. cinerea* hyphae treated with eosin Y to stain chitosan after 24 h of competition with the *P. putida* KT2440 WT and *Pseudomonas* 250 J WT strains and strains carrying plasmids (p2213, p2213-VgrG2a-csn and p2213-VgrG250 J-csn). The reduction in the eosin Y signal during competition with KT2440 and 250 J carrying p2213-VgrG250 J-csn indicates chitosan degradation. Scale = 10 µm. **B** Box-and-whisker plot showing the relative signal intensity of eosin Y for *B. cinerea* (prey) growing alone and in competition with the KT2440 WT or 250 J WT strain and strains carrying plasmids (p2213-VgrG2a-csn and p2213-VgrG250 J-csn) as attackers. **C** Representative TEM images of *B. cinerea* under different conditions: control, competing with KT2440 wildtype, KT2440 (p2213-VgrG250 J-csn), 250 J wildtype, and 250 J (p2213-VgrG250 J-csn). The images show disruption of the beta-glucan layer when *B. cinerea* interacts with strains expressing chitosanase. Scale bars are included in the images. At least 5 hyphae ($N = 5$) were analyzed in all the cases, and the error bars represent the SDs. Statistical significance was assessed via one-way ANOVA. **** p value < 0.0001

To eliminate the possibility of chitosanase being released in a T6SS-independent manner from the cells, we performed competition assays using KT2440 Δ3T6SS, lacking the three T6SSs encoded in the WT genome, as the delivery bacterium (Suppl. Figure 5 A and B). Eosin Y staining of chitosan from *B. cinerea* after competition with these strains revealed no detrimental effect on chitosan degradation, thus confirming that the observed chitosanase activity was dependent on the presence of a functional T6SS.

Ultimately, we aimed to explore the potential of using an alternative bacterial background for the T6SS-dependent release of effectors and proteins of interest. To validate our system in other microbial delivery systems, we used *Pseudomonas* sp. 250 J, a strain with beneficial effects on plants [55], with two T6SSs encoded in its genome and up to 15 T6SS-dependent effectors. The results obtained in competition assays between *B. cinerea* and *Pseudomonas* sp. 250 J (WT and carrying plasmids expressing VgrGs and Csn) showed the same behavior

as that observed with KT2440 (Fig. 4A and B), thus confirming the specificity between chitosanase and VgrG250 J and the activity of this combination in different genetic backgrounds.

To further support these observations, we performed TEM assays to directly visualize the structural damage induced in *B. cinerea* during bacterial-fungal competition. As shown in Fig. 4C and Suppl. Figure 5 C, the secretion of chitosanase via a functional T6SS led to severe fungal cell wall disruption, particularly affecting the β-glucan layer and overall wall integrity. This structural damage was notably pronounced when *B. cinerea* was in competition with KT2440 or 250 J strains expressing the VgrG250 J-csn construct, in comparison to interactions with WT strains. These findings complement the quantitative data obtained from Eosin Y staining, reinforcing the notion that T6SS-mediated chitosanase secretion enhances antifungal activity against *B. cinerea.*

Discussion

Bacteria employ a wide arsenal of molecular systems and metabolites to compete for nutrients and space and to interact positively or negatively with other microbes and higher organisms. One such system described in Gram-negative bacteria is the T6SS, which, under certain conditions, provides a competitive advantage over the other members of the ecological niche inhabited by these microbes [56, 57].

This work presents a strategy to apply basic knowledge developed about T6SSs to complement classic approaches to combat microbes via the use of genetically engineered T6SSs. In addition, this approach opens up the possibility of selecting different bacterial delivery strains depending on the environmental context or specific needs of the crop. By integrating the engineered T6SS system into beneficial bacterial strains, we can tailor biocontrol strategies to particular ecological niches, thus optimizing the performance of strains in agricultural environments. To do so, in this work we selected the well-known soil bacterium *P. putida* KT2440 as the delivery bacterial system because of its genetic and ecological versatility. Furthermore, *Pseudomonas* sp. 250 J has also been proven to be a promising delivery strain since this strain also shows biocontrol and plant growth-promoting (PGP) properties [55]. To provide additional antibacterial and antifungal properties to delivery bacteria, inducible and constitutive expression plasmids carrying different T6SS-dependent effectors have been used (Figs. 1, 2 and 3). Our results confirm the inhibitory effects initially described for these toxins against other microbes, such as Tfe2 against *S. cerevisiae* or TplE against *E. coli* [18, 46]. Moreover, our findings demonstrate that the engineered T6SS system can also target fungal cells, as evidenced by the cellular damage observed in *B. cinerea* when competing with KT2440 expressing Tfe2 (Fig. 3C). These results highlight the versatility of the T6SS as a tool for microbial interference, extending its potential applications beyond bacterial competition to fungal biocontrol strategies.

In addition, the engineered system we developed and tested demonstrates the possibility of releasing non-T6SS-related effectors such as chitosanase, a protein involved in the degradation of chitosan, in a T6SS-dependent manner (Fig. 4). The release of T6SS- and non-T6SS-related proteins by this system opens a wide array of possibilities for applications, not only in agriculture, such as via inhibition of *B. cinerea* growth, but also in other scientific fields, as it could be possible to release specific proteins directly into the cytoplasm of target cells, thus facilitating their entry and increasing their efficacy. In addition, this system provides a series of advantages over other platforms, such as the direct delivery of effectors and proteins into the cytoplasm or its broad spectrum of target cells ranging from eukaryotic to prokaryotic cells. However, potential limitations of using noncanonical T6SS effectors include size constraints affecting their secretion, intrinsic toxicity to the delivery bacterium, and stability issues in complex environments. Additionally, precise pairing with T6SS structural components may require further optimization. Future advancements in protein engineering and bioinformatics will be critical for addressing these challenges and enhancing the versatility of T6SS-based systems.

This work also highlights the relevance of the specificity and modularity of T6SSs. For the efficient release of effectors in a T6SS-dependent manner, cargo effectors are usually covalently or noncovalently linked to VgrG, PAAR or Hcp proteins [58]. The use of different VgrGs led us to compare the functionality of VgrGs within a phylogenetically related T6SS framework, providing insights into whether effector secretion efficiency is influenced by VgrG-T6SS specificity. The correct pairing of VgrG and PAAR proteins with their respective effectors was critical for achieving effective antimicrobial activity. Our results demonstrated that not all the combinations were functional, such as the combination of VgrG2a from *P. aeruginosa* with chitosanase, which showed no activity. However, other combinations have been successful, such as the one between the nonrelated VgrGkt4 from *P. putida* KT2440 with TplE from *P. aeruginosa*. This highlights the importance of understanding the intricate relationships between the structural components of the T6SS and the effector.

In future applications, careful design of these pairings, or the use of modified evolved VgrGs, could allow expansion of the use of T6SS to target specific pathogens in diverse environmental or clinical settings. The use of

inducible promoters with different levels of strength will help to modulate the effector expression level and optimize the performance of the genetic system. In addition, as demonstrated in Fig. 2, the use of artificial intelligence (AI) and bioinformatic tools designed to study protein–protein interactions, such as Alphaphold3, will be helpful for the determination of possible effector–VgrG/PAAR/Hcp interactions to develop more successful combinations, which will lead to increased efficiencies. However, while this approach has successfully highlight tip protein (VgrG/PAAR) and effector interactions in many cases, no conclusive results have been shown in other cases as was the case of VgrG250 J with chitosanase and even with interactions already described in bibliography, therefore, although interesting and useful, it must be used cautiously to avoid misunderstandings.

Owing to its versatility, the T6SS can be engineered not only to eliminate pathogens but also to promote the proliferation of organisms or to modulate complex populations. For example, its application in soils or plant leaves could be interesting for the modification of plant microbiomes by targeting harmful bacteria or fungi or favoring the growth of a specific bacterium by enhancing its resistance to biotic and abiotic stressors [59]. To achieve this level of precision, T6SS platforms must be equipped with tailored sets of effectors. Our work demonstrates the potential of engineered T6SS systems to deliver not only traditional T6SS effectors but also noncanonical T6SSs, broadening the range of molecules that can be deployed.

The application of this promising genetic tool in combination with omic approaches will lead to the discovery of multiple T6SS effectors for the 'à la carte' customization of biocontrol strains for application against pathogens and for the study of defense mechanisms against these kinds of effectors. This offers a novel approach in which the T6SS functions as a versatile delivery system, increasing the efficacy of these effectors against specific microbial targets with minimal changes in the environment and other microbial populations. This provides opportunity for innovative applications, ranging from personalized medical treatments to the enhancement of soil health in agriculture, all of which are based on the precise manipulation of microbial ecosystems.

Conclusions

This study successfully demonstrates the feasibility of engineering *P. putida* KT2440 as a delivery system for T6SS-dependent effectors, highlighting its potential as a biocontrol agent against bacterial and fungal phytopathogens. We demonstrate the successful secretion of both canonical T6SS effectors and non-T6SS-related proteins, significantly expanding the functional repertoire of this secretion system. Specifically, we provide *P. putida* KT2440 with novel antibacterial effectors against Gram-positive and Gram-negative bacteria, leading to bacterial cell death and ROS induction and cellular damages on fungi. Finally, we demonstrate that non-T6SS-related proteins, such as chitosanase, can be T6SS-dependently secreted for chitosan degradation.

In summary, these findings emphasize the adaptability of the T6SS for diverse biotechnological applications. The engineered T6SS demonstrates great promise for combating microbial pathogens, manipulating microbial ecosystems, and enabling precision microbial engineering in sustainable agriculture, environmental management, and therapeutic development.

Supplementary Information

The online version contains supplementary material available at https://doi.org/10.1186/s13036-025-00497-w.

Supplementary Material 1: Suppl. Table 1. Bacterial strains used in this work.

Supplementary Material 2: Suppl. Table 2. Oligonucleotides used in this study.

Supplementary Material 3: Suppl. Figure 1. Schematic representation of the bacterial competition assay setup between bacterial strains. Created with BioRender.

Supplementary Material 4: Suppl. Figure 2. Schematic representations of inducible plasmids carrying effectors. A) Schematic representation of the p234 plasmid carrying *paar* (orange) and *tse1* (green) from *P. chlororaphis*. pSEVA plasmid expression is controlled by the lacI-Ptrc promoter. B) Schematic representation of the p238 plasmid carrying *vgrGkt4* (orange) and *tplE-tplEi-PA1508* (green) from *P. aeruginosa* PAO1. pSEVA plasmid expression is controlled by the xylS-Pm promoter.

Supplementary Material 5: Suppl. Figure 3. Interkingdom competitions mediated by T6SS effectors. A) CLSM of *B. cinerea* hyphae after competition with *P. putida* KT2440 WT and carrying plasmids (p234-VgrG1-Tfe2 and p234-VgrG2-Tfe2). The samples were treated with FM4-64 and DHR 123 to stain the fungal membrane and reactive oxygen species, respectively. FM4-64 penetration into the cytoplasm is indicative of cell death. Scale = 10 µm.

Supplementary Material 6: Suppl. Figure 4. Interkingdom competitions mediated by T6SS effectors. A) CLSM of *B. cinerea* hyphae after competition with the*P. putida* KT2440 (Δ3T6SS) strain or strains carrying plasmids (p234-VgrG1-Tfe2 and p234-VgrG2-Tfe2) as attackers. The samples were treated with FM4-64 and DHR123 to stain the fungal membrane and reactive oxygen species, respectively. Scale = 10 µm. B) Box-and-whisker plot showing the mean ROS pixel intensity (a.u.) of *B. cinerea* (prey) growing alone and in competition with the *P. putida* KT2440 (Δ3T6SS) strain or strains carrying plasmids (p234-VgrG1-Tfe2 and p234-VgrG2-Tfe2). as attackers. In all the experiments, at least three biological replicates are shown, and the error bars represent the SDs. Statistical significance was assessed via one-way ANOVA. **** *p* value <0.0001. C) TEM analysis of *B. cinerea* (prey) growing alone and in competition with the KT2440 WT strain and strains carrying plasmids (p234-Tfe2 and p234-VgrG1-Tfe2). Scale = 1 µm.

Supplementary Material 7: Suppl. Figure 5. Interkingdom competitions mediated by non-T6SS-dependent effectors. A) CLSM of *B. cinerea* hyphae treated with eosin Y to stain chitosan after 24 h of competition with the *P. putida* KT2440 (Δ3T6SS) strain and strains carrying plasmids (p2213-VgrG2a-csn and p2213-VgrG250J-csn). The lack of a reduction in the eosin Y signal during competition is indicative of the absence of chitosanase activity. Scale = 10 µm. B) Box-and-whisker plot showing the relative signal intensity of eosin Y for *B. cinerea* (prey) growing alone and

in competition with the *P. putida* KT2440 (Δ3T6SS) strain and strains carrying plasmids (p2213-VgrG2a-csn and p2213-VgrG250J-csn) as attackers. C) Representative TEM images of *B. cinerea* under different conditions: control, competing with KT2440 wildtype, KT2440 (p2213-VgrG250J-csn), 250J wildtype, and 250J (p2213-VgrG250J-csn). The images show severe cellular damage when *B. cinerea* interacts with strains expressing chitosanase. Scale bars are included in the images. At least 8 hyphae ($N = 8$) were analyzed in all the cases, and the error bars represent the SDs. Statistical significance was assessed via one-way ANOVA.

Acknowledgements
We thank Saray Morales for technical support. We also thank Alicia Esteban and David Navas from the IHSM and SCAI microscopy units, respectively, for their technical support in confocal microscopy. We are grateful to Esteban Martínez-García from the CNB (Madrid, Spain) for providing SEVA plasmids from SEVA collection. This work was supported by grant from Consolidación Investigadora (CSN2022 - 135744). A.I.P.L. is funded by the program FPU (FPU19/00289) and the program Plan Propio de Investigación y Transferencia from Universidad de Málaga.

Adherence to national and international regulations
Not applicable.

Authors' contributions
C.M.S conceived the study; C.M.S designed the experiments; C.M.S., A.I.P.L and M.A. performed the main experimental work; C.M.S wrote the manuscript; and A.I.P.L, D.R. and A.V contributed critically to writing the final version of the manuscript.

Funding
This work was supported by grant from Consolidación Investigadora (CSN2022 - 135744). A.I.P.L. is funded by the program FPU (FPU19/00289) and the program Plan Propio de Investigación y Transferencia from Universidad de Málaga.

Data availability
The data supporting the findings of this study are available from the corresponding author (camolsan@uma.es) upon request.

Declarations

Ethics approval and consent to participate
Not applicable.

Consent for publication
All authors have seen and approved the submission of the manuscript.

Competing interests
The authors declare no competing interests.

Received: 12 December 2024 Accepted: 26 March 2025
Published online: 03 April 2025

References

1. Hibbing ME, Fuqua C, Parsek MR, Peterson SB. Bacterial competition: surviving and thriving in the microbial jungle. Nat Rev Microbiol. 2010;8(1):15–25.
2. Stubbendieck RM, Vargas-Bautista C, Straight PD. Bacterial Communities: Interactions to Scale. Front Microbiol. 2016;7:1234.
3. Granato ET, Meiller-Legrand TA, Foster KR. The Evolution and Ecology of Bacterial Warfare. Curr Biol. 2019;29(11):R521–37.
4. Niehaus L, Boland I, Liu M, Chen K, Fu D, Henckel C, et al. Microbial coexistence through chemical-mediated interactions. Nat Commun. 2019;10(1):2052.
5. Peterson SB, Bertolli SK, Mougous JD. The Central Role of Interbacterial Antagonism in Bacterial Life. Curr Biol. 2020;30(19):R1203–14.
6. Martin JF, Casqueiro J, Liras P. Secretion systems for secondary metabolites: how producer cells send out messages of intercellular communication. Curr Opin Microbiol. 2005;8(3):282–93.
7. Blasey N, Rehrmann D, Riebisch AK, Muhlen S. Targeting bacterial pathogenesis by inhibiting virulence-associated Type III and Type IV secretion systems. Front Cell Infect Microbiol. 2022;12:1065561.
8. Fronzes R, Christie PJ, Waksman G. The structural biology of type IV secretion systems. Nat Rev Microbiol. 2009;7(10):703–14.
9. Lasica AM, Ksiazek M, Madej M, Potempa J. The Type IX Secretion System (T9SS): Highlights and Recent Insights into Its Structure and Function. Front Cell Infect Microbiol. 2017;7:215.
10. Russell AB, Hood RD, Bui NK, LeRoux M, Vollmer W, Mougous JD. Type VI secretion delivers bacteriolytic effectors to target cells. Nature. 2011;475(7356):343–7.
11. Mougous JD, Cuff ME, Raunser S, Shen A, Zhou M, Gifford CA, et al. A virulence locus of *Pseudomonas aeruginosa* encodes a protein secretion apparatus. Science. 2006;312(5779):1526–30.
12. Pukatzki S, Ma AT, Sturtevant D, Krastins B, Sarracino D, Nelson WC, et al. Identification of a conserved bacterial protein secretion system in *Vibrio cholerae* using the *Dictyostelium* host model system. Proc Natl Acad Sci U S A. 2006;103(5):1528–33.
13. Hood RD, Peterson SB, Mougous JD. From Striking Out to Striking Gold: Discovering that Type VI Secretion Targets Bacteria. Cell Host Microbe. 2017;21(3):286–9.
14. Basler M, Pilhofer M, Henderson GP, Jensen GJ, Mekalanos JJ. Type VI secretion requires a dynamic contractile phage tail-like structure. Nature. 2012;483(7388):182–6.
15. Silverman JM, Brunet YR, Cascales E, Mougous JD. Structure and regulation of the type VI secretion system. Annu Rev Microbiol. 2012;66:453–72.
16. Cianfanelli FR, Alcoforado Diniz J, Guo M, De Cesare V, Trost M, Coulthurst SJ. VgrG and PAAR Proteins Define Distinct Versions of a Functional Type VI Secretion System. PLoS Pathog. 2016;12(6): e1005735.
17. Cianfanelli FR, Monlezun L, Coulthurst SJ. Aim, Load, Fire: The Type VI Secretion System, a Bacterial Nanoweapon. Trends Microbiol. 2016;24(1):51–62.
18. Trunk K, Peltier J, Liu YC, Dill BD, Walker L, Gow NAR, et al. The type VI secretion system deploys antifungal effectors against microbial competitors. Nat Microbiol. 2018;3(8):920–31.
19. Molina-Santiago C, Pearson JR, Navarro Y, Berlanga-Clavero MV, Caraballo-Rodriguez AM, Petras D, et al. The extracellular matrix protects *Bacillus subtilis* colonies from *Pseudomonas* invasion and modulates plant co-colonization. Nat Commun. 2019;10(1):1919.
20. Perez-Lorente AI, Molina-Santiago C, de Vicente A, Romero D. Sporulation Activated via sigma(W) Protects *Bacillus* from a Tse1 Peptidoglycan Hydrolase Type VI Secretion System Effector. Microbiol Spectr. 2023;11(2): e0504522.
21. Ren A, Jia M, Liu J, Zhou T, Wu L, Dong T, et al. Acquisition of T6SS Effector TseL Contributes to the Emerging of Novel Epidemic Strains of *Pseudomonas aeruginosa*. Microbiol Spectr. 2023;11(1): e0330822.
22. Allsopp LP, Bernal P. Killing in the name of: T6SS structure and effector diversity. Microbiology (Reading). 2023;169(7).
23. Bondage DD, Lin J-S, Ma L-S, Kuo C-H, Lai E-M. VgrG C terminus confers the type VI effector transport specificity and is required for binding with PAAR and adaptor–effector complex. 2016;113(27):E3931-E40.
24. Flaugnatti N, Le TTH, Canaan S, Aschtgen M-S, Nguyen VS, Blangy S, et al. A phospholipase A1 antibacterial Type VI secretion effector interacts directly with the C-terminal domain of the VgrG spike protein for delivery. 2016;99(6):1099–118.
25. Shneider MM, Buth SA, Ho BT, Basler M, Mekalanos JJ, Leiman PG. PAAR-repeat proteins sharpen and diversify the type VI secretion system spike. Nature. 2013;500(7462):350–3.
26. Alcoforado Diniz J, Liu YC, Coulthurst SJ. Molecular weaponry: diverse effectors delivered by the Type VI secretion system. Cell Microbiol. 2015;17(12):1742–51.
27. Durand E, Nguyen VS, Zoued A, Logger L, Pehau-Arnaudet G, Aschtgen MS, et al. Biogenesis and structure of a type VI secretion membrane core complex. Nature. 2015;523(7562):555–60.

28. Jana B, Fridman CM, Bosis E, Salomon D. A modular effector with a DNase domain and a marker for T6SS substrates. Nat Commun. 2019;10(1):3595.
29. Wood TE, Howard SA, Wettstadt S, Filloux A. PAAR proteins act as the "sorting hat" of the type VI secretion system. Microbiology (Reading). 2019;165(11):1203–18.
30. Liang X, Pei TT, Li H, Zheng HY, Luo H, Cui Y, et al. VgrG-dependent effectors and chaperones modulate the assembly of the type VI secretion system. PLoS Pathog. 2021;17(12): e1010116.
31. Pukatzki S, Ma AT, Revel AT, Sturtevant D, Mekalanos JJ. Type VI secretion system translocates a phage tail spike-like protein into target cells where it cross-links actin. Proc Natl Acad Sci U S A. 2007;104(39):15508–13.
32. Wettstadt S, Lai EM, Filloux A. Solving the Puzzle: Connecting a Heterologous Agrobacterium tumefaciens T6SS Effector to a *Pseudomonas aeruginosa* Spike Complex. Front Cell Infect Microbiol. 2020;10:291.
33. Flaugnatti N, Le TT, Canaan S, Aschtgen MS, Nguyen VS, Blangy S, et al. A phospholipase A1 antibacterial Type VI secretion effector interacts directly with the C-terminal domain of the VgrG spike protein for delivery. Mol Microbiol. 2016;99(6):1099–118.
34. Ma LS, Hachani A, Lin JS, Filloux A, Lai EM. Agrobacterium tumefaciens deploys a superfamily of type VI secretion DNase effectors as weapons for interbacterial competition in planta. Cell Host Microbe. 2014;16(1):94–104.
35. Kamal F, Liang X, Manera K, Pei TT, Kim H, Lam LG, et al. Differential Cellular Response to Translocated Toxic Effectors and Physical Penetration by the Type VI Secretion System. Cell Rep. 2020;31(11): 107766.
36. Jana B, Keppel K, Salomon D. Engineering a customizable antibacterial T6SS-based platform in *Vibrio natriegens*. EMBO Rep. 2021;22(11): e53681.
37. Hersch SJ, Lam L, Dong TG. Engineered Type Six Secretion Systems Deliver Active Exogenous Effectors and Cre Recombinase. mBio. 2021;12(4):e0111521.
38. Ting SY, Martinez-Garcia E, Huang S, Bertolli SK, Kelly KA, Cutler KJ, et al. Targeted Depletion of Bacteria from Mixed Populations by Programmable Adhesion with Antagonistic Competitor Cells. Cell Host Microbe. 2020;28(2):313–21 e6.
39. Bernal P, Llamas MA, Filloux A. Type VI secretion systems in plant-associated bacteria. Environ Microbiol. 2018;20(1):1–15.
40. de Lorenzo V, Perez-Pantoja D, Nikel PI. *Pseudomonas putida* KT2440: the long journey of a soil-dweller to become a synthetic biology chassis. J Bacteriol. 2024;206(7): e0013624.
41. Weimer A, Kohlstedt M, Volke DC, Nikel PI, Wittmann C. Industrial biotechnology of *Pseudomonas putida*: advances and prospects. Appl Microbiol Biotechnol. 2020;104(18):7745–66.
42. Martínez-García E, Fraile S, Algar E, Aparicio T, Velázquez E, Calles B, et al. SEVA 4.0: an update of the Standard European Vector Architecture database for advanced analysis and programming of bacterial phenotypes. Nucleic Acids Research. 2022;51(D1):D1558-D67.
43. Gibson DG, Young L, Chuang RY, Venter JC, Hutchison CA 3rd, Smith HO. Enzymatic assembly of DNA molecules up to several hundred kilobases. Nat Methods. 2009;6(5):343–5.
44. Choi KH, Kumar A, Schweizer HP. A 10-min method for preparation of highly electrocompetent *Pseudomonas aeruginosa* cells: application for DNA fragment transfer between chromosomes and plasmid transformation. J Microbiol Methods. 2006;64(3):391–7.
45. Schindelin J, Arganda-Carreras I, Frise E, Kaynig V, Longair M, Pietzsch T, et al. Fiji: an open-source platform for biological-image analysis. Nat Methods. 2012;9(7):676–82.
46. Jiang F, Wang X, Wang B, Chen L, Zhao Z, Waterfield NR, et al. The *Pseudomonas aeruginosa* Type VI Secretion PGAP1-like Effector Induces Host Autophagy by Activating Endoplasmic Reticulum Stress. Cell Rep. 2016;16(6):1502–9.
47. Abramson J, Adler J, Dunger J, Evans R, Green T, Pritzel A, et al. Accurate structure prediction of biomolecular interactions with AlphaFold 3. Nature. 2024;630(8016):493–500.
48. Álvarez-Salmoral D, Borza R, Xie R, Joosten RP, Hekkelman ML, Perrakis A. AlphaBridge: tools for the analysis of predicted macromolecular complexes. bioRxiv. 2024:2024.10.23.619601.
49. Guerra RM, Maleno FD, Figueras MJ, Pujol-Bajador I, Fernandez-Bravo A. Potential Pathogenicity of *Aeromonas* spp. Recovered in River Water, Soil, and Vegetation from a Natural Recreational Area. Pathogens. 2022;11(11).
50. Richards JK, Xiao CL, Jurick WM, 2nd. Botrytis spp.: A Contemporary Perspective and Synthesis of Recent Scientific Developments of a Widespread Genus that Threatens Global Food Security. Phytopathology. 2021;111(3):432–6.
51. DEAN R, VAN KAN JAL, PRETORIUS ZA, HAMMOND-KOSACK KE, DI PIETRO A, SPANU PD, et al. The Top 10 fungal pathogens in molecular plant pathology. Molecular Plant Pathology. 2012;13(4):414–30.
52. Storey D, McNally A, Åstrand M, sa-Pessoa Graca Santos J, Rodriguez-Escudero I, Elmore B, et al. *Klebsiella pneumoniae* type VI secretion system-mediated microbial competition is PhoPQ controlled and reactive oxygen species dependent. PLOS Pathogens. 2020;16(3):e1007969.
53. Santos-Moriano P, Kidibule PE, Alleyne E, Ballesteros AO, Heras A, Fernandez-Lobato M, et al. Efficient conversion of chitosan into chitooligosaccharides by a chitosanolytic activity from *Bacillus thuringiensis*. Process Biochem. 2018;73:102–8.
54. Baker LG, Specht CA, Donlin MJ, Lodge JK. Chitosan, the Deacetylated Form of Chitin, Is Necessary for Cell Wall Integrity in *Cryptococcus neoformans*. Eukaryot Cell. 2007;6(5):855–67.
55. Molina-Santiago C, Udaondo Z, Ramos J-L. Draft whole-genome sequence of the antibiotic-producing soil isolate *Pseudomonas* sp. strain 250J. Environmental Microbiology Reports. 2015;7(2):288–92.
56. Yang X, Liu H, Zhang Y, Shen X. Roles of Type VI Secretion System in Transport of Metal Ions. Front Microbiol. 2021;12: 756136.
57. Chen L, Zou Y, Kronfl AA, Wu Y. Type VI secretion system of *Pseudomonas aeruginosa* is associated with biofilm formation but not environmental adaptation. MicrobiologyOpen. 2020;9(3): e991.
58. Li Y, Yan X, Tao Z. Two Type VI Secretion DNase Effectors are Utilized for Interbacterial Competition in the Fish Pathogen *Pseudomonas plecoglossicida*. Front Microbiol. 2022;13: 869278.
59. Perez-Lorente AI, Romero D, Molina-Santiago C. Unravelling the impact of environmental factors in shaping plant microbiomes. Microb Biotechnol. 2024;17(6): e14504.

Publisher's Note